Macromolecules
ARTICLE

Macromolecules **2010**, *43*, 2925–2932 **2925**
DOI: 10.1021/ma1000546

Crystalline Phase of Isomorphic Poly(hexamethylene sebacate-*co*-hexamethylene adipate) Copolyester: Effects of Comonomer Composition and Crystallization Temperature

Zhichao Liang, Pengju Pan, Bo Zhu, Tungalag Dong, Lei Hua, and Yoshio Inoue*

Department of Biomolecular Engineering, Tokyo Institute of Technology, 4259-B-55 Nagatsuta, Midori-ku, Yokohama 226-8501, Japan

Received August 7, 2009; Revised Manuscript Received February 9, 2010

ABSTRACT: The crystalline phase of random poly(hexamethylene sebacate-*co*-hexamethylene adipate) (P(HSe-*co*-HA)) was studied by differential scanning calorimetry (DSC), Fourier transform infrared (FTIR) spectroscopy, wide-angle X-ray diffraction (WAXD), and small-angle X-ray scattering (SAXS). From the quantitative analysis of the comonomer composition in the crystalline phase and the finding of the change both in the WAXD patterns and in the *d*-spacing values of some planes in the HA composition (C_{HA}) of 60 mol % $< C_{HA} <$ 70 mol %, the occurrence of isodimorphism was confirmed for P(HSe-*co*-HA). As the secondary comonomer unit content in the crystalline phase decreased with increasing crystallization temperature, it was concluded that the cocrystallization of the HSe and HA units in the crystal of P(HSe-*co*-HA) is affected by kinetics. From SAXS analysis, the lamella thickness of P(HSe-*co*-HA) was found to rely on the comonomer unit inclusion behavior in the PHSe or PHA type crystal. Application of the Sanchez−Eby model suggests low values of excess free energy of inclusion in PHSe or PHA type crystal, indicating that the cocrystallization of HSe and HA units in the crystal of P(HSe-*co*-HA) is thermodynamically favored.

Introduction

Aliphatic polyesters have received considerable interest over recent decades, for their expected biodegradability and their potential application in biomedical field.[1] As an important kind of aliphatic polyesters, poly(alkylene dicarboxylate)s were the first polymers synthesized by well-understood reaction chemistry and also were the first such polymers that their crystalline structures have been studied by X-ray diffraction.[2] The recent studies indicate that the crystalline structure of poly(alkylene dicarboxylate)s, especially, the chain conformation in the crystalline phase, depends on the methylene contents of both diacid and diol units.[3−9] When the methylene content in the ester units is low, such as those derived from ethylene glycol, 1,4-butanediol, succinic acid, and adipic acid,[3−9] polyesters tend to deviate from the all-trans conformation and adopt a twist conformation[10] or gauche conformations.[11] However, if the methylene content of both aliphatic diol and dicarboxylic units is high, the aliphatic polyesters adopt a quasi-all-trans conformation.[8,12] Hence, these poly(alkylene dicarboxylate)s with high methylene content tend to form similar crystalline structures, especially the similar values of *d*-spacing of characteristic planes, such as the planes of (110), (020), (120), and (200),[4−8,10] if they have similar chemical structure. In the two-component random aliphatic copolyesters, if the two comonomers have similar chemical structures and occupy approximately the same volume, the cocrystallization of these comonomer units may be expected, since the excess free energy for cocrystallization of the comonomer units into the same crystalline lattice is very low, and the chain conformations of the corresponding comonomer segments become compatible with either crystalline lattice.[13]

*To whom corresponding should be addressed: Tel +81-45-924-5794; Fax +81-45-924-5827; e-mail inoue.y.af@m.titech.ac.jp.

Comonomers of some random aliphatic copolyesters, such as poly(butylene succinate-*co*-ethylene succinate) (P(BS-*co*-ES)),[14] poly(butylenes succinate-*co*-propylene succinate) (P(BS-*co*-PS),[15] and poly(hexamethylene sebacate-*co*-hexamethylene adipate) (P(HSe-*co*-HA)),[16] do cocrystallize. The P(BS-*co*-ES)s[14] and P(BS-*co*-PS)s[15] showed isodimorphic cocrystallization, where either the crystalline lattice of comonomers was adopted below or above the eutectic point. Particularly, the cocrystallization of P(HSe-*co*-HA) reported by Li et al.[16] is of interest. The parent homopolymers, PHSe and PHA, have different crystalline structures (PHSe: monoclinic unit cell, containing two chains, with a = 0.544 nm, b = 0.730 nm, c = 2.20 nm, and β = 113.3°;[10] PHA: orthorhombic unit cell, containing eight chains, with a = 1.008 nm, b = 1.464 nm, and c = 1.683 nm[17]). They do not seem to meet the requirements of cocrystallization very well. In addition, the cocrystallization of P(HSe-*co*-HA) copolymers seems to be different from the case of isomorphism in a strict sense or isodimorphism. Its lattice parameters were found to change discontinuously and become relatively large with the comonomer unit composition. Moreover, despite the HSe unit has a larger size than the HA unit (in chemistry), the crystalline structure of copolymer is much more sensitive with the incorporation of, even a small amount of, the HA units than that of the HSe unit. These unique cocrystallization behaviors make it worthy of a further understanding of the cocrystallization mechanism of P(HSe-*co*-HA)s. It is expected that more extensive studies of a series of P(HSe-*co*-HA) copolymers may enable us to obtain the comprehensive picture of cocrystallization in copolymer systems.

The solid-state properties of copolyesters are affected by the minor component in the crystalline phase of copolymers.[18] Therefore, it is of interest to quantify the comonomer composition in the crystalline phase. Several theories for copolymer crystallization have been developed, which are reasonably classified into two types: the comonomer exclusion model[19−21] and the

Published on Web 02/17/2010

Table 1. Feed Molar Ratios of Monomer in Reactor, Comonomer Composition in Copolymers, Molecular Weight Parameters, Melting Temperatures, Heat of Fusion, and Degree of Crystallinity of P(HSe-*co*-HA)s

sample code (molar ratio HSe/HA)	SA/AA[a] molar ratio in feed	HSe/HA molar ratio in copolymer[b]	M_n[c]	M_w[c]	PDI[c]	T_m[d] (°C)	ΔH_m[d] (J/g)	crystallinity[e] (%)
100/0	100/0	100/0	1.1×10^4	1.5×10^4	1.36	68.9	110	60
90/10	90.6/9.4	88.6/11.4	1.0×10^4	1.4×10^4	1.40	64.2	109	59
80/20	80.3/19.7	81.9/18.1	1.6×10^4	2.3×10^4	1.44	62.0	88	59
70/30	69.7/30.3	68.5/31.5	1.2×10^4	1.6×10^4	1.33	57.7	91	57
50/50	49.8/50.2	48.8/51.2	1.2×10^4	1.7×10^4	1.42	54.5	81	57
40/60	40.5/59.5	41.4/58.6	1.8×10^4	2.5×10^4	1.38	49.7	81	50
30/70	29.4/70.6	27.9/72.1	1.0×10^4	1.5×10^4	1.50	50.4	88	52
20/80	20.3/79.7	20.8/79.2	1.6×10^4	2.4×10^4	1.50	54.1	77	45
0/100	0/100	0/100	1.5×10^4	2.2×10^4	1.47	59.2	81	45

[a] SA, sebacic acid; AA, adipic acid. [b] Comonomer-unit composition of P(HSe-*co*-HA) was estimated by ^{1}H NMR analysis, $\delta = \pm 2\%$; the fraction numbers indicate the molar ratio of HSe/HA in the whole copolymer (see S-1 in the Supporting Information). [c] M_n, M_w, and PDI were measured by GPC analysis. [d] T_m and ΔH_m were obtained by DSC at a heating rate of 10 °C/min. [e] The crystallinity was measured by WAXD, with error range of ±5%.

comonomer inclusion model.[22−24] Particularly, the pragmatic treatment of Sanchez and Eby[23] was recommended by Crist.[25] The Sanchez−Eby theory is correct for observed final melting temperatures T_m' of lamellar crystals with thickness l_{max}, without any need for extrapolation to "equilibrium".[25] The required basal surface energy σ and heat of fusion ΔH_m^0 for lamellar crystals that melt at $T_m' = T_m(l_{max})$ are in all probability the same as for homopolymer crystals. Furthermore, there is no need to assume complete exclusion of comonomer as with Flory theory.[19,25] The estimation of comonomer content in the crystalline phase based on the experimental results and theoretical calculations of the excess free energy are helpful for interpreting the copolymer melting temperature.[25]

IR spectra are sensitive to the conformation and packing state of molecular chains. Thus, they have been widely exploited to characterize semicrystalline polymers in terms of crystallinity,[26] such as the crystallinity of poly(ε-caprolactone) (PCL),[27] and the quantitative analysis of copolymer systems or their blends.[28,29] The quantitative FTIR method is also available for determination of comonomer composition in the crystalline phase in the present study if the IR spectra of the crystalline phase are resolvable.

In this work, in order to comprehensively understand the cocrystallization of copolymer systems, we shall investigate the crystalline phase of P(HSe-*co*-HA). The thermal behavior of P(HSe-*co*-HA) was investigated with differential scanning calorimetry (DSC). The crystalline structure of P(HSe-*co*-HA) was analyzed by Fourier transform infrared (FTIR) spectroscopy, wide-angle X-ray diffraction (WAXD), and small-angle X-ray scattering (SAXS). The thermodynamic analysis based on the Sanchez−Eby model[23] enables a further understanding about the cocrystallization behavior of these copolyesters.

Experimental Section

Materials. PHSe, PHA, and their copolymer P(HSe-*co*-HA) were synthesized from hexanediol, sebacic acid, and adipic acid with various feeding molar ratios of sebacic acid (SA)/adipic acid (AA) in a 250 mL three-neck flask with an oil−water separator, according to the polycondensation method reported by Li et al.[16] The products were purified by the dissolving−precipitating method with chloroform/ethanol before filtrating and dried at 60 °C under vacuum for 24 h. The number- and weight-average molecular weights (M_n, M_w) and their distributions (polydispersity index: PDI) of polyester samples were determined by gel permeation chromatography (GPC) system (Tosoh Co., Tokyo, Japan). The comonomer compositions of the copolymers were determined using ^{1}H NMR and ^{13}C NMR techniques. Both the 600 MHz ^{1}H and 150 MHz ^{13}C NMR spectra were recorded on a Bruker AVANCE 600 spectrometer (Bruker BioSpin K.K, Osaka, Japan) using deuteriochloroform ($CDC1_3$) as the solvent. The chemical shifts reported were referenced to internal tetramethylsilane (0.00 ppm) or the solvent resonance at the appropriate frequency.

DSC. The isothermal and nonisothermal crystallization behavior of the polymer samples were investigated by a Pyris Diamond differential scanning calorimeter (DSC) (Perkin-Elmer Japan Corp., Yokohama, Japan) under a nitrogen atmosphere. The scales of temperature and heat flow at different heating rates were calibrated using an indium standard. The samples were weighted and sealed in an aluminum pan. In the nonisothermal melt crystallization, the samples were melted at 100 °C for 2 min before being cooled to −50 °C under a cooling rate of 10 °C/min. An intracooler was connected to the DSC apparatus to achieve reliability at high cooling rates over the whole temperature range of the experiments.

FTIR Spectroscopy. The copolymer samples were observed on an FTIR spectrometer (JASCO International Co. Ltd., Tokyo, Japan) equipped with an AIM-8800 multichannel infrared microscope (JASCO International Co. Ltd., Tokyo, Japan) and a MCT detector in the transmission mode. P(HSe-*co*-HA) sample was placed between two pieces of BaF_2 slides, and then it was melted at 100 °C for 2 min before quenched to the desired T_c. For studying the crystalline structure, the FTIR spectra of all crystallized samples were measured at 25 °C to erase the temperature effect on the IR spectra. After the melt-crystallization, the sample was heated from T_c to 100 at 1 °C/min in a LK-600FTIR hot stage (Japan High Tech Co., Ltd., Fukuoka, Japan) for studying the melting behavior. The FTIR spectra were recorded at a 1 °C interval during the heating process, and the spectra were collected with 32 scans and a resolution of 2 cm^{-1}.

X-ray Analysis. The crystalline structure of polymer sample was investigated by WAXD and SAXS analysis with a Rigaku RU-200 (Rigaku Corp., Tokyo, Japan), working at 40 kV and 200 mA, with Ni-filtered Cu Kα radiation ($\lambda = 0.154\,18$ nm). WAXD patterns were recorded in the 2θ range of 5°−50° at a scanning rate of 2°/min. Assuming that the diffraction peaks from a crystallographic plane and the amorphous halo could be reproduced by a Gaussian curve and a sum of two Gaussian curves, respectively, diffraction patterns in the 2θ range of 5°−50° were resolved into a series of Gaussian peaks by curve-fitting using the damped least-squares algorithm. The degree of crystallinity was calculated from the relative areas of the resolved peaks. SAXS profiles were recorded in the 2θ range 0.1°−2.5°. Each step increased 2θ by 0.04°, and X-rays were collected for 4 s at each step. The samples for the WAXD and SAXS analysis were prepared by hot-press at 100 °C before complete crystallization at 25 °C.

Results and Discussion

Characterization of Copolymers. Table 1 summarizes the results for the characterization of copolymers. As shown in

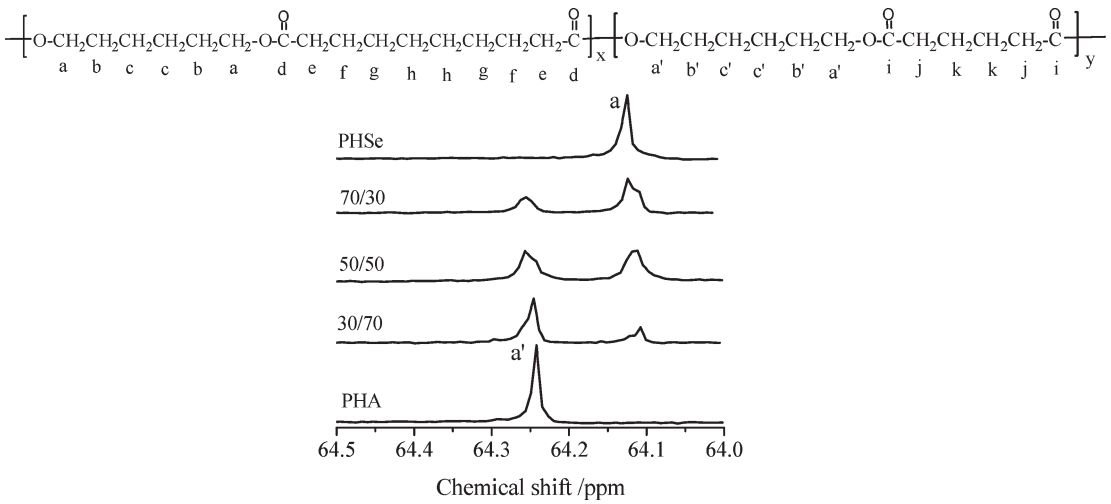

Figure 1. 600 MHz ^{13}C NMR spectrum of PHSe, PHA, and P(HSe-*co*-HA)s at the 64.5−64.0 ppm region; 70/30, 50/50, and 30/70 denote P(HSe-*co*-HA)(70/30), P(HSe-*co*-HA)(50/50), and P(HSe-*co*-HA)(30/70), respectively.

Table 2. Distribution of Selected Triads for P(HSe-*co*-HA) Copolymers

		AHA[b] (%)		AHS + SHA[b] (%)		SHS[b] (%)	
sample[a]	HSe/HA molar ratio in polymer	obsd[c]	calcd[d]	obsd[c]	calcd[d]	obsd[c]	calcd[d]
90/10	88.6/11.4	1.4	1.3	21.0	20.2	77.6	78.5
80/20	81.9/18.1	3.2	3.3	28.0	29.6	68.8	67.1
70/30	68.5/31.5	9.4	9.9	41.6	43.2	49.0	46.9
50/50	48.8/51.2	22.7	26.2	50.0	50.0	27.3	23.8
40/60	41.4/58.6	33.6	34.4	49.0	48.5	17.4	17.1
30/70	27.9/72.1	51.0	52.0	39.8	40.2	9.2	7.8
20/80	20.8/79.2	66.2	62.8	29.2	32.9	4.6	4.3

[a] The fraction numbers denote the feed molar ratio of HSe/HA in the copolymers. [b] Unit abbreviations: AHA, AHS, SHA, and SHS denote the units of adipate−hexamethylene−adipate, adipate−hexamethylene−sebacate, sebacate−hexamethylene−adipate, and sebacate−hexamethylene−sebacate, respectively. [c] Measured from the ^{13}C NMR by curve-fitting. [d] Calculated for a random P(HSe-*co*-HA) copolymer.

this table, a comparison between feed molar ratios of monomers and comonomer composition in copolymers indicates clearly that they are in excellent agreement with each other. Hence, the comonomer composition of P(HSe-*co*-HA) can be easily controlled by adjusting the monomer feed ratio. Here, the samples are referenced using the feed molar ratios of monomer units for simplicity. PHSe, PHA, P(HSe-*co*-HA)(90/10), P(HSe-*co*-HA)(80/20), P(HSe-*co*-HA)(70/30), P(HSe-*co*-HA)(50/50), P(HSe-*co*-HA)(40/60), P(HSe-*co*-HA)(30/70), and P(HSe-*co*-HA)(20/80) were synthesized in this study, with an error range of estimated composition of ±2%.

^{13}C NMR has been proved to be effective in determining the repeating unit sequence distributions in the macromolecular chains.[30] The comonomer sequence distribution of P(HSe-*co*-HA) copolymers was determined using ^{13}C NMR spectroscopy. As shown in Figure 1, the ^{13}C resonances at 64.24 and 64.13 ppm are assigned to the methylene carbon *a*′ in PHA and methylene carbon *a* in PHSe, respectively. Moreover, in the ^{13}C NMR spectra of copolymer samples, the resonance of carbons *a*′ and *a* were found to be the superposition of the resonances at 64.26, 64.24 ppm and those at 64.13 and 64.11 ppm, which may be respectively assigned to the carbon *a*′ in the adipate−hexamethylene−sebacate (AHS) and the adipate−hexamethylene−adipate (AHA) units and the carbon *a* in the sebacate−hexamethylene−sebacate (SHS) and the sebacate−hexamethylene−adipate (SHA) units. By integrating corresponding resonances, the ratios of AHA to AHS/SHA to SHS triads were estimated for all the P(HSe-*co*-HA) copolymers, as shown in Table 2. Meanwhile, the relative distributions of AHA, AHS/SHA, and SHS triads in statistically random P(HSe-*co*-HA) copolymers are also calculated and summarized in Table 2. The good agreement between the experimental and the theoretically calculated values for P(HSe-*co*-HA) copolymers may indicate that all of the prepared P(HSe-*co*-HA) samples are nearly random copolymers. Details of ^{1}H and ^{13}C NMR analysis and calculation are provided as S-1 and S-2 in the Supporting Information.

DSC Analysis. At first, the nonisothermal melt crystallization at a cooling rate of 10 °C/min and the subsequent melting process at a heating rate of 10 °C/min are investigated by DSC for PHSe, PHA, and P(HSe-*co*-HA)(90/10, 80/20, 70/30, 50/50, 40/60, 30/70, 20/80), as shown in Figure 2. The obtained peak melting temperature T_c and the heat of fusion ΔH_m are summarized in Table 1. Each copolymer sample shows a single exothermal peak and an endothermal peak in the melt−crystallization process and the subsequent heating process, respectively. The values of ΔH_m of all P(HSe-*co*-HA) samples are higher than 70 J/g, indicating the high crystallinity is established during the melt crystallization. This is a strong evidence for occurrence of cocrystallization of the HSe and HA comonomer units into the same crystalline lattice.

Moreover, as shown in Figure 3, both the crystallization and melting temperature of P(HSe-*co*-HA) copolymers display a composition-dependent behavior. A systematic crystallization and melting temperature depression can be observed with increasing comonomer compositions, while the lowest crystallization and melting temperatures are observed at C_{HA} = 60 mol %, i.e., P(HSe-*co*-HA)(40/60), where C_{HA} indicates the HA unit content in the bulk

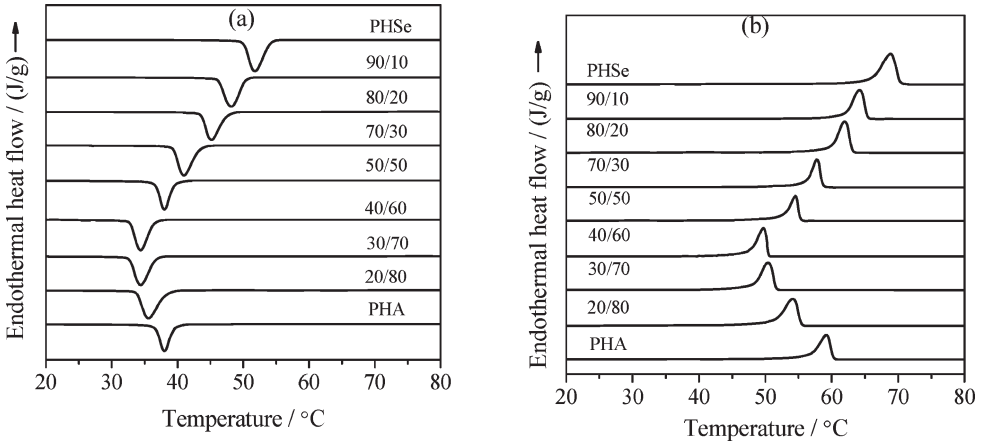

Figure 2. DSC thermodiagrams of P(HSe-*co*-HA) samples in (a) nonisothermal melt−crystallization at a cooling rate of 10 °C/min and (b) the subsequent melting process at a heating rate of 10 °C/min.

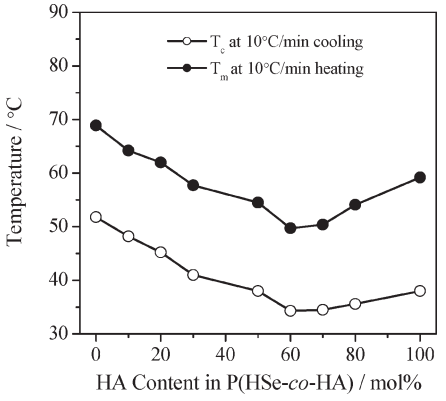

Figure 3. Curves of T_c and T_m vs HA content in copolymer.

copolymer. For the case of cocrystallization of comonomer units in the crystal, these results may indicate the isodimorphism of the random copolymers.[13,31]

FTIR Analysis. The cocrystallization of P(HSe-*co*-HA) can be further confirmed by the in situ measurement of FTIR. At first, the characteristic absorption bands of crystals were identified for PHSe and PHA. The infrared spectra of PHSe, PHA, and P(HSe-*co*-HA) and their second derivative observed at 25 °C are presented in Figure 4. The bands at 1464, 1416, 1398, 1371, 1264, 1176, 972, 921, 911, and 735 cm^{-1} for PHA and bands at 1467, 1415, 1401, 1378, 1361, 1294, 1220, 1174, 977, 917, 857, and 753 cm^{-1} for PHSe show significant intensity increase with the time elapse in the melt−crystallization process. This indicates that the changes in the chain conformation caused by ordered chain packing during crystallization.[16] Especially, the bands at 1264, 921, and 911 cm^{-1} for PHA and those at 1294, 1220, 917, and 857 cm^{-1} for PHSe appear only in the crystalline state, and all disappear in the melt. Hence, it is reasonable to assign them as the characteristic bands for the crystalline state of PHA and PHSe, respectively. Furthermore, in the in situ FTIR measurements of P(HSe-*co*-HA) copolyesters in the melt−crystallization and the subsequent melting process of samples, all the intensities of these characteristic bands of PHA and PHSe synchronously increase with time in the crystallization process, decrease in the heating process, and finally disappear in the melt. This result provides the further evidence for the cocrystallization of the HSe and the HA comonomers units in these P(HSe-*co*-HA) copolyesters.[16]

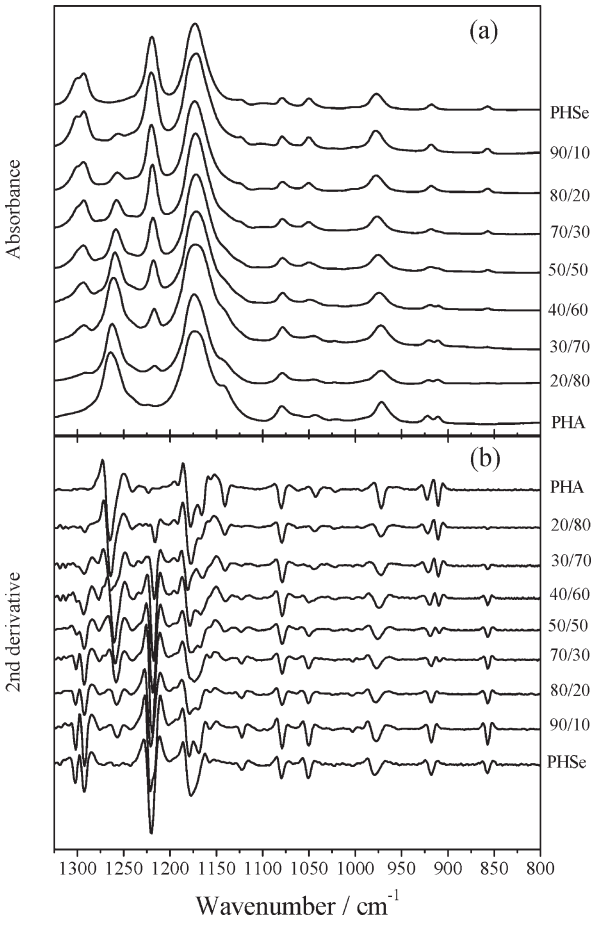

Figure 4. (a) IR spectra in the 1325−800 cm^{-1} region of P(HSe-*co*-HA)s crystallized at 25 °C and (b) the second derivative of the IR spectra.

It is also interesting to find that the position of these characteristic crystalline bands almost remained unchanged despite the variation of the comomoner composition in P(HSe-*co*-HA)s. This may indicate that the HA and HSe comonomer units in P(HSe-*co*-HA) copolymers maintained their chain conformation or packing state in the crystalline state as if they were in the crystalline phase of the HA or HSe homopolymers, since the IR spectrum is sensitive to the conformation and the packing state of the molecular chains.

Table 3. Assignments of IR Bands of PHA and PHSe in the Crystalline Phase[a] (for 1500−800 cm^{-1})

PHA		PHSe	
υ/cm^{-1}	assignment[a,b,c]	υ/cm^{-1}	assignment[a,b,c]
735	$\gamma_r(CH_2)$	753	$\gamma_r(CH_2)$
911, 921, 972	υ(C−C)	857, 917, 977	υ(C−C)
1176	υ(OC−O)	1174	υ(OC−O)
1264	υ_{as}(C−O−C)	1220	υ_{as}(C−O−C)
1371, 1398	$\gamma_w(CH_2)$	1294	γ_w(C−O + C−C)
1416, 1464	$\delta(CH_2)$	1361, 1378, 1401	$\gamma_w(CH_2)$
		1415, 1467	$\delta(CH_2)$

[a] All the IR bands are assigned for only the crystalline phase. [b] υ = stretching, γ_w = wagging, γ_r = rocking, δ = bending, υ_{as} = asymmetric stretching. [c] The chemical groups in the parentheses indicate the assigned groups.

Furthermore, we can make the assignments of many IR bands referring to those of polyethylene (PE),[32] PCL,[33,34] poly(lactic acid) (PLA),[35] poly(3-hydroxypropionate) (P(3HP)),[36] poly(butylenes succinate) (PBS),[37] and poly(butylene adipate) (PBA),[38] as summarized in Table 3. According to these assignments, the crystallization of the polymer can be more efficiently followed by the FTIR measurement.

Comonomer-Unit Composition in the Crystalline Phase of P(HSe-*co*-HA). The comonomer-unit composition in the crystalline phase of P(HSe-*co*-HA) can be determined from the IR spectra according to the Beer−Lambert law, as eq 1, and eq 2 which is deduced from this law for P(HSe-*co*-HA) systems (see S-3 in the Supporting Information)

$$A_c = bc\int_0^{+\infty} \varepsilon(\upsilon)\,d\upsilon \quad (1)$$

where A_c is the integrated intensity A of a characteristic band, ε is the absorption coefficient, b is the thickness, c is the concentration, υ is the wavenumber of the characteristic band.

$$X_{HA} = \frac{c_{HA}}{c_{HA} + c_{HSe}} = \frac{A_{921}}{A_{917}/\varepsilon(917/921) + A_{921}} \quad (2)$$

Here, X_{HA} is the HA content in the crystalline phase, A_{917} and A_{921} denote the integrated intensity of characteristic crystalline bands at 917 and 921 cm^{-1}, respectively, and ε(917/921) is the relative absorption coefficient of the characteristic bands at 917 and 921 cm^{-1}, i.e., $\varepsilon(917/921) = \varepsilon(917)/\varepsilon(921)$. The value of ε(917/921) was estimated to be 1.146 for P(HSe-*co*-HA)s. Details of calculation are provided as S-3 in the Supporting Information.

Some previous researches, such as the extensive study on the crystallization of the isodimorphous P(3HB-*co*-3HV),[18,39−41] have already shown that the comonomer-unit content in the crystalline phase is strongly dependent on the copolymer composition and the crystallization conditions.[42,43] Therefore, we studied the influence of both the HA unit content, C_{HA}, in the bulk copolymer and the crystallization temperature, T_c, on the relative content of the HA unit, X_{HA}, in the crystalline phase of P(HSe-*co*-HA) in order to obtain an intensive comprehension of the cocrystallization of P(HSe-*co*-HA).

The IR spectra in the region of 950−800 cm^{-1} were analyzed quantitatively to investigate the comonomer-unit content in the crystalline phase of P(HSe-*co*-HA) samples crystallized at 25 °C. In Figure 5, the results of X_{HA} were plotted against the C_{HA}. The solid line represents the X_{HA}−C_{HA} relationship expected by the uniform inclusion model, i.e., $X_{HA} = C_{HA}$, and the dotted line represents the X_{HA} value of 50 mol %. As shown in Figure 5, the values of X_{HA} in the crystal of P(HSe-*co*-HA) increased as C_{HA} is increased from 0 to 100 mol %. Moreover, for C_{HA} lower or higher than about 60 mol %, the values of X_{HA} were found to be lower or higher than that expected from the "uniform inclusion" model respectively, i.e., $X_{HA} < C_{HA}$ ($C_{HA} \leq 60$ mol %) and $X_{HA} > C_{HA}$ ($C_{HA} \geq 60$ mol %). Since it is more difficult for the secondary component to be included in the crystalline region of the main component,[18,26] this result indicates the transformation of the dominant monomer unit in the crystalline region from the HSe unit to the HA unit as the C_{HA} value increased from 60 to 70 mol %.

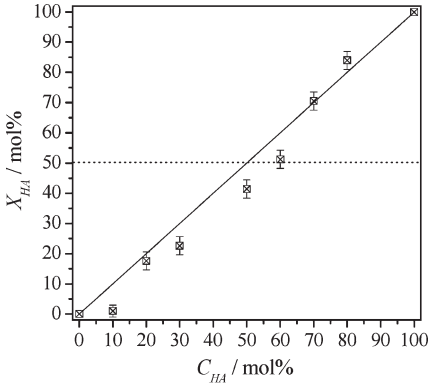

Figure 5. Relative HA content X_{HA} in the crystalline phase as a function of the HA unit content C_{HA} in the bulk copolymer.

As found by DSC measurements, the deepest depression of melting temperature was found in the vicinity of C_{HA} = 60 mol %, which is expected to be the transition point of different types of crystals.[13] Hence, these two results can be regarded as the evidence for the isodimorphism of P(HSe-*co*-HA) with the actual isodimorphic crossover among the C_{HA} value of 60−70 mol %; i.e., for $C_{HA} \leq 60$ mol % the copolymers form the PHSe type lattice, and for $C_{HA} \geq$ 70 mol % they form the PHA type lattice.

The IR spectra of P(HSe-*co*-HA) samples crystallized at different T_c were quantitatively analyzed in order to study the effect of crystallization condition on the crystallization of P(HSe-*co*-HA). Parts a and b of Figure 6 show the X_{HA} values plotted against T_c for P(HSe-*co*-HA)s with the PHSe type crystal and those with the PHA type crystal, respectively. After the isothermal crystallization at the temperature ranged from 25 to 55 °C, the value of X_{HA} remained lower than 5 mol % for P(HSe-*co*-HA)(90/10) while it retained around 50 mol % for P(HSe-*co*-HA)(40/60). Meanwhile, for P(HSe-*co*-HA)(80/20), P(HSe-*co*-HA)(70/30), and P(HSe-*co*-HA)(50/50), the values of X_{HA} tend to slightly decrease with increasing T_c without regard to the possible error of the data. On the other hand, Figure 6b shows that the X_{HA} value increased with the crystallization temperature for samples with the PHA type crystal. These results demonstrate that the lattice of the dominant comonomer units tends to have less inclusion of the secondary units as crystallization temperature increases, indicating that the cocrystallization of P(HSe-*co*-HA) at deep undercooling is affected by kinetics. Moreover, the curves of X_{HA} vs T_c appear to "flatten out" at shallower undercoolings, suggesting that a thermodynamic analysis might be worthwhile for the cocrystallization of these copolymers.

WAXD Analysis. Though the unit cell parameters of PHA (a = 1.008 nm, b = 1.464 nm, c = 1.683 nm)[17] and PHSe (a = 0.544 nm, b = 0.73 nm, c = 2.2 nm, and β = 113.3°)[10] seem to be totally different, it is interesting to find that the d-spacing values of (110), (020), (120), and (200) for PHSe are

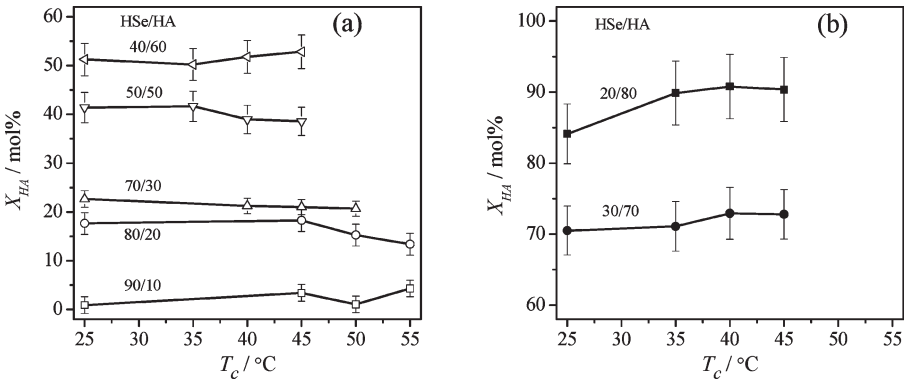

Figure 6. Relative HA content X_{HA} in the crystalline phase as a function of crystallization temperature T_c: (a) P(HSe-*co*-HA) with $C_{HA} \leq 60$ mol %; (b) P(HSe-*co*-HA) with $C_{HA} \geq 70$ mol %. The feed molar ratio HSe/HA of the copolymers is shown in the figures.

Table 4. Value of *d*-Spacing of the Characteristic Planes of PHA and PHSe from WAXD

PHA[a]		PHSe[b]	
index	d_{measd}[c] (nm)	index	d_{measd}[c] (nm)
220	0.415 vs	110	0.411 vs
040	0.366 vs	020	0.365 vs
240	0.296 w	120	0.295 w
400	0.252 s	200	0.250 m

[a] From ref 17. [b] From ref 10. [c] Abbreviation denote relative intensities: vs, very strong; s, strong; m, medium; w, weak.

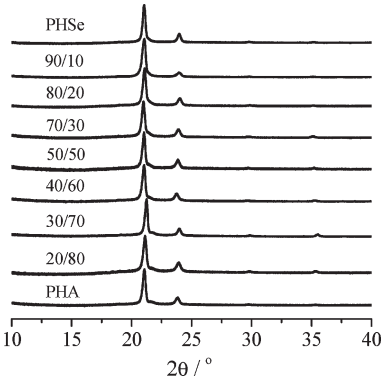

Figure 7. WAXD patterns of P(HSe-*co*-HA) crystallized at 25 °C.

very close to those of (220), (040), (240), and (400) for PHA, respectivley,[7,10,17] as shown in Table 4. The all-trans conformation has been proposed for PHSe and the diol segment of PHA, although a kink one has been proposed for the diacid segment of PHA, which may result in the slightly different *d*-spacing values between PHA and PHSe.[7,10,17] As noted by Li et al.,[16] the spacing values of *d*(220), *d*(040), *d*(240), and *d*(400) obtained from the WAXD result for the crystal of P(HSe-*co*-HA) are close to those of PHSe and PHA, indicating the similar crystalline structure of these polymers. This is consistent with the WAXD results of PHSe and PHA in our study.

In Figure 7 are shown the WAXD patterns for P(HSe-*co*-HA) copolymers. The patterns of PHSe, PHA, and their copolyesters P(HSe-*co*-HA) are quite similar to each other. Clear crystalline diffractions in the WAXD can be observed for all P(HSe-*co*-HA) copolymer samples. The difference in the WAXD patterns between P(HSe-*co*-HA)(40/60) and P(HSe-*co*-HA)(30/70) is small but significant. Especially, the peak positions shifted to lower angle side as C_{HA} increases from 70 to 100 mol %.

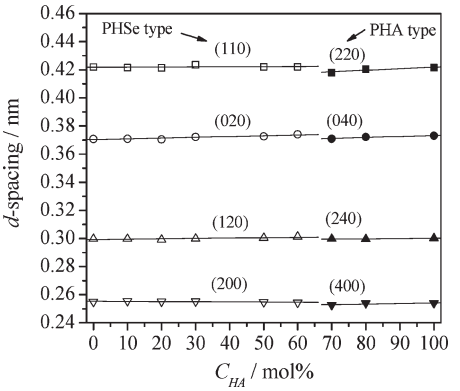

Figure 8. WAXD *d*-spacing of the characteristic planes as a function of the HA unit content C_{HA} in the bulk copolymer. The PHSe type and PHA type lattice were assigned according to refs 10 and 17, respectively.

The *d*-spacing values of the crystalline planes were calculated with the Bragg equation based on these WAXD patterns. In Figure 8, the plots of *d*-spacing vs HA content (mole fraction) were presented for (220), (040), (240), and (400) planes (the PHA type crystal) and (110), (020), (120), and (200) planes (the PHSe type crystal). These crystalline planes were assigned according to the study of PHSe and PHA.[10,17] As shown in Figure 8, with increasing the C_{HA} value from 0 to 60 mol %, *d*(110) seldom changed around 0.422 nm, while *d*(020) increased from 0.370 to 0.374 nm. On the other hand, when the C_{HA} value increased from 70 to 100 mol %, *d*(220) increased from 0.418 to 0.422 nm while *d*(040) increased from 0.370 to 0.373 nm. These results indicate that different types of lattice were formed for copolymers with the C_{HA} value higher or lower than 60 mol %. Hence, the WAXD results further support the isodimorphism of P(HSe-*co*-HA) and confirm that the composition for transition of crystal type is about 60−70 mol % of the HA units content.

The degree of crystallinity of samples can be determined from the WAXD patterns using the relative areas under the crystalline peaks and the amorphous background. As summarized in Table 1, the degree of crystallinity of the P(HSe-*co*-HA) samples are ca. 44.5−60.5%. Such high degrees of crystallinity, observed over a wide range of comonomer composition, indicate the occurrence of cocrystallization in the whole composition of P(HSe-*co*-HA). Moreover, the crystallinity was found to be dependent on the comonomer composition. Particularly, the crystallinity at $C_{HA} = 60$ mol % was the lowest among the samples with the PHSe type crystal. This may be due to the significant exclusion of the

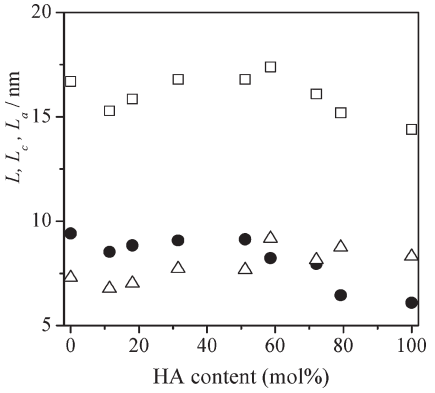

Figure 9. Long period L (□), lamella thickness L_c (●), and amorphous thickness L_a (△) of P(HSe-*co*-HA) as a function of HA content.

HA units from the lattice of the PHSe type crystal, since the X_{HA} value is much lower than the C_{HA} value although the C_{HA} value is higher than that of C_{HSe} at C_{HA} = 60 mol %. Meanwhile, the crystallinity at C_{HA} = 70 mol % was the highest among the samples with the PHA type crystal. It should be ascribed to the high-level inclusion of the HSe unit in the PHA type crystal because the value of X_{HA} is rather close to that expected from the uniform inclusion at C_{HA} = 70 mol %. These denote the well agreement between the WAXD results and the quantitative analysis of IR spectra.

SAXS Analysis. The long period, L, was determined from the maximum of the first-order correlation function estimated from the SAXS patterns. Two maxima were observed in the Lorentz-corrected SAXS profiles, while the ratio of the angular positions of the second and first scattering maximum was relatively close to 2.00 for all P(HSe-*co*-HA) samples. As demonstrated by Crist et al.,[44] it is well justified to use the first scattering maximum to calculate the average structural period of the lattice (long period) in such conditions. The long periods were then given by the Bragg relation. Assuming a simple two-phase model of the lamella morphology, the lamella thickness, L_c, and the amorphous layer thickness, L_a, can be estimated by the product of L and the volume fraction of crystal, χ_v, which is calculated from the mass fraction of the crystal, χ_m. It is safe to assume that $\chi_m \approx \chi_w$ since the electron density is approximately proportional to the mass. Hence, χ_v is determined from eq 3[41]

$$\chi_v = \frac{\rho^a}{(1-\chi_w)\rho^c + \chi_w \rho^a}\chi_w \qquad (3)$$

where ρ^a and ρ^c are the amorphous and crystalline densities, respectively. The amorphous and crystalline densities of PHSe at 25 °C were reported to be 1.033 and 1.151 g cm^{-3}, respectively, and those of PHA to be 1.096 and 1.222 g cm^{-3}.[6,7]

The amorphous density ρ^a for P(HSe-*co*-HA) copolymers was estimated as the density of the blend of amorphous PHSe and PHA. The amorphous density ρ^a at 25 °C for P(HSe-*co*-HA)s with PHSe and PHA type crystal can be determined by plotting ρ^a(PHSe type) and ρ^a(PHA type) against C_{HA} and C_{HSe}, respectively. The results are ρ^a(PHSe type) = 1.040 + 0.065C_{HA} and ρ^a(PHA type) = 1.096 − 0.069C_{HSe}, respectively. Therefore, we estimated lamella thickness L_c as a product of L and χ_v and the thickness of the amorphous layer L_a as $L - L_c$.[41]

The data of L_c and L_a together with L for P(HSe-*co*-HA)s were plotted as a function of the HA content in Figure 9. At low HA content, the incorporation of HA comonomer units in the PHSe type crystal results in the decrease of L, L_c, and L_a. This trend is similar to the case of P(HB-*co*-HV).[41] In the P(HSe-*co*-HA) of low HA content, relatively long HSe sequences are abundant, and the entropy gain upon the cocrystallization is little. Therefore, there should be a marked tendency for the HA units to be excluded from the lamella to the lamella surface where the distortion of the crystalline lattice upon the inclusion of the HA units can be easily relaxed. Both L and L_a increase with the further increase of the HA content, while L_c increases as the HA content increases from 10 to 50 mol %, but significantly decreases at the HA content of 60 mol %, which is consistent with the drop in crystallinity at 60 mol % HA. For the copolymers forming the PHA type crystal, both L and L_c increase with increasing the HSe content, while L_a is almost invariant. The dependence of crystallinity and L_c on the comonomer composition may be partly due to the change in the degree of supercooling, since the melting temperature of P(HSe-*co*-HA)s depressed with increasing comonomer content. However, the more important reason for such dependence should be the inclusion of comonomer units in the host lamella, which is also the reason for the depression of melting temperature with increasing comonomer content in P(HSe-*co*-HA)s. Therefore, the inclusion of comonomer units in the crystal of the main component enables the increase of both the lamella thickness and the crystallinity, while the exclusion results in a decrease in the lamella thickness.

Moreover, the inclusion of comonomer units in PHSe or PHA type crystal was further studied with the Sanchez−Eby model. Sanchez and Eby[23] followed the approach of Helfand and Lauritzen[22] for including the comonomer units within the crystal of main component in copolymer and also extended the analysis of copolymer melting to the lamellar crystals of finite thickness l_{max}. The Sanchez−Eby model[23] is given as eq 4

$$T_m(l)\left\{1 + \frac{RT_m^0}{\Delta H^\circ}\left[(1-X_c)\ln\left[\frac{1-X_c}{1-X}\right] + X_c \ln\left[\frac{X_c}{X}\right]\right]\right\} = T_m^0\left[1 - \frac{2\sigma_e}{\Delta H^\circ}(1/l) - \frac{E}{\Delta H^\circ}X_c\right] \qquad (4)$$

where $T_m(l)$ denotes the melting temperature of thin crystals and l is the thickness of the crystalline layer ($l = L_c$), T_m^0 and ΔH° are respectively the equilibrium melting temperature and enthalpy of the homopolymer, X_c and X (mole fraction, $X = C_{HA}$ or C_{HSe} in this study) denote respectively the comonomer content in the crystalline phase and in the whole copolymer, and σ_e and E are respectively the fold surface free energy and the excess free energy of incorporating comonomer units in the host crystalline lattice.

Both the values of lamellar thickness l (L_c) and the comonomer content in the crystalline phase of copolymer have been determined for P(HSe-*co*-HA)s. Hence, the values of σ_e and E, as the average values in the PHSe or PHA type crystal, can be estimated from eq 4. The average values of σ_e and E for P(HSe-*co*-HA)s forming the PHSe type crystal were determined to be 3.99 kJ/(mol of folds) and 3.31 kJ/mol, respectively, while those for copolymers forming PHA type crystal were estimated to be 3.37 kJ/(mol of fold) and 2.75 kJ/mol, respectively. Particularly, the low E values suggest that the inclusion of comonomer units in the lamella is thermodynamically favored. Moreover, the E value of inclusion in PHA type crystal is lower than that in the PHSe type crystal, denoting the inclusion of HSe units in the PHA type crystal is easier than the incorporation of HA units in the PHSe type crystal. This is consistent with the result of the quantitative analysis of IR spectra.

Conclusion

In this study of the crystalline phase of random P(HSe-*co*-HA) copolymers, depression of crystallization and melting temperatures was observed with increasing comonomer compositions, while the lowest crystallization and melting temperatures were observed at C_{HA} = 60 mol %. From the quantitative analysis of the comonomer composition in the crystalline phase and the finding of change both in the WAXD patterns and in the *d*-spacing values of some planes within composition of 60 mol % < C_{HA} < 70 mol %, the occurrence of isodimorphism was confirmed for P(HSe-*co*-HA). As the comonomer-unit content in the crystalline phase decreased with increasing crystallization temperature, it was concluded that the cocrystallization of the HSe and HA units in the same crystal of P(HSe-*co*-HA) is affected by kinetics. From SAXS analysis, the lamella thickness of P(HSe-*co*-HA) was found to rely on the comonomer-unit inclusion behavior in the PHSe or PHA type crystal. The low values of excess free energy (*E*) for inclusion of the comonomer units in the PHSe or PHA type crystal, as estimated with the Sanchez−Eby model, suggest that the cocrystallization of HSe and HA in the crystal of P(HSe-*co*-HA) is thermodynamically favored. Moreover, the lower value of *E* in PHA than in PHSe type crystal denotes the inclusion of HSe units in the PHA type crystal is easier than the incorporation of HA units in the PHSe type crystal.

Supporting Information Available: Determination of the compositions of P(HSe-*co*-HA)s with ^{1}H NMR technology; determination of the distribution of repeating unit sequence of P(HSe-*co*-HA)s with ^{13}C NMR technology; determination of the comonomer content in the crystalline phase of P(HSe-*co*-HA)s. This material is available free of charge via the Internet at http://pubs.acs.org.

References and Notes

(1) Pan, P.; Inoue, Y. *Prog. Polym. Sci.* **2009**, *34*, 605–640.
(2) Fuller, C. S. *Chem. Rev.* **1940**, *26*, 143–167.
(3) Turner-Jones, A.; Bunn, C. W. *Acta Crystallogr.* **1962**, *15*, 105–113.
(4) Ueda, A. S.; Chatani, Y.; Tadokoro, H. *Polym. J.* **1971**, *2*, 387–397.
(5) Minke, R.; Blackwell, J. *J. Macromol. Sci., Phys.* **1979**, *B16*, 407–417.
(6) Aylwin, P. A.; Boyd, R. H. *Polymer* **1984**, *25*, 323–329.
(7) Kanamoto, T.; Tanaka, K. *J. Polym. Sci., Part A-2* **1971**, *9*, 2043–2060.
(8) Ihn, K. J.; Yoo, E. S.; Im, S. S. *Macromolecules* **1995**, *28*, 2460–2464.
(9) Liau, W. B.; Boyd, R. H. *Macromolecules* **1990**, *23*, 1539–1544.
(10) Armelin, E.; Casas, M. T.; Puiggalí, J. *Polymer* **2001**, *42*, 5695–5699.
(11) Alemán, C.; Puiggalí, J. *J. Org. Chem.* **1997**, *62*, 3076–3080.
(12) Fuller, C. S. *J. Am. Chem. Soc.* **1939**, *61*, 2575–2580.
(13) Allegra, G.; Bassi, I. W. *Adv. Polym. Sci.* **1969**, *6*, 549–574.
(14) Mochizuki, M.; Mukai, K.; Yamada, K.; Ichise, N.; Murase, S.; Iwaya, Y. *Macromolecules* **1997**, *30*, 7403–7407.
(15) Papageorgiou, G. Z.; Bikiaris, D. N. *Biomacromolecules* **2007**, *8*, 2437–2449.
(16) Li, X.; Sun, J.; Huang, Y.; Geng, Y.; Wang, X.; Ma, Z.; Shao, C.; Zhang, X.; Yang, C.; Li, L. *Macromolecules* **2008**, *41*, 3162–3168.
(17) Gestí, S.; Almontassir, A.; Casas, M. T.; Puiggalí, J. *Biomacromolecules* **2006**, *7*, 799–808.
(18) Kamiya, N.; Sakurai, M.; Inoue, Y.; Chûjô, R. *Macromolecules* **1991**, *24*, 3888–3892.
(19) Flory, P. J. *J. Chem. Phys.* **1947**, *15*, 684.
(20) Flory, P. J. *Trans. Faraday Soc.* **1955**, *51*, 848–857.
(21) Baur, V. H. *Makromol. Chem.* **1966**, *98*, 297–301.
(22) Helfand, E.; Lauritzen, J. I. *Macromoelcules* **1973**, *6*, 631–638.
(23) Sanchez, I. C.; Eby, R. K. *Macromolecules* **1975**, *8*, 638–641.
(24) Wendling, J.; Suter, U. W. *Macromolecules* **1998**, *31*, 2516–2520.
(25) Crist, B. *Polymer* **2003**, *44*, 4563–4572.
(26) Hagemann, H.; Snyder, R. G.; Peacock, A. J.; Mandelkern, L. *Macromolecules* **1989**, *22*, 3600–3606.
(27) He, Y.; Inoue, Y. *Polym. Int.* **2000**, *49*, 623–626.
(28) Fei, B.; Chen, C.; Wu, H.; Peng, S.; Wang, X.; Dong, L. *Eur. Polym. J.* **2003**, *39*, 1939–1946.
(29) Buback, M.; Busch, M.; Dröge, T.; Mahling, F.; Prellberg, C. *Eur. Polym. J.* **1997**, *33*, 375–379.
(30) Jiang, Z. *Biomacromolecules* **2008**, *9*, 3246–3251.
(31) Jeong, Y. G.; Jo, W. H.; Lee, S. C. *Macromolecules* **2000**, *33*, 9705–9711.
(32) Krimm, S.; Liang, C. Y.; Sutherlan, G. B. B. M. *J. Chem. Phys.* **1956**, *25*, 549–562.
(33) Yan, C.; Li, H. H.; Zhang, J. M.; Ozaki, Y.; Shen, D. Y.; Yan, D. D.; Shi, A. C.; Yan, S. K. *Macromolecules* **2006**, *39*, 8041–8048.
(34) Elzein, T.; Nasser-Eddine, M.; Delaite, C.; Bistac, S.; Dumas, P. *J. Colloid Interface Sci.* **2004**, *273*, 381–387.
(35) Kister, G.; Cassanas, G.; Vert, M. *Polymer* **1998**, *39*, 267–273.
(36) Zhu, B.; Kai, W.; Pan, P.; Yazawa, K.; Nishida, H.; Sakurai, M.; Inoue, Y. *J. Phys. Chem. B* **2008**, *112*, 9684–9692.
(37) Ichikawa, Y.; Washiyama, J.; Moteki, Y.; Noguchi, K.; Okuyama, K. *Polym. J.* **1995**, *27*, 1230–1238.
(38) Yan, C.; Zhang, Y.; Hu, Y.; Ozaki, Y.; Shen, D.; Gan, Z.; Yan, S.; Takahashi, I. *J. Phys. Chem. B* **2008**, *112*, 3311–3314.
(39) Kamiya, N.; Sakurai, M.; Inoue, Y.; Chûjô, R. *Macromolecules* **1991**, *24*, 2178–2182.
(40) Kamiya, N.; Sakurai, M.; Inoue, Y.; Chûjô, R. *Macromolecules* **1992**, *25*, 2046–2048.
(41) Yoshie, N.; Saito, M.; Inoue, Y. *Macromolecules* **2001**, *34*, 8953–8960.
(42) VanderHart, D.; Orts, W. J.; Marchessault, R. H. *Macromolecules* **1995**, *28*, 6394–6400.
(43) Orts, W. J.; Marchessault, R. H.; Bluhm, T. L. *Macromolecules* **1991**, *24*, 6435–6438.
(44) Crist, B.; Morosoff, N. *J. Polym. Sci., Polym. Phys. Ed.* **1973**, *11*, 1023–1045.